

Universal Negative Energetic Elasticity in Polymer Chains: Crossovers among Random, Self-Avoiding, and Neighbor-Avoiding Walks

Nobu C. Shirai^{1,*} and Naoyuki Sakumichi^{2,†}

¹Center for Information Technologies and Networks, Mie University, Tsu, Mie 514-8507, Japan

²Department of Chemistry and Biotechnology, The University of Tokyo, Bunkyo-ku, Tokyo 113-8656, Japan

(Dated: August 28, 2024)

Negative energetic elasticity in gels challenges the conventional understanding of gel elasticity, and despite extensive research, a concise explanation remains elusive. In this Letter, we use the weakly self-avoiding walk (the Domb–Joyce model; DJ model) and interacting self-avoiding walk (ISAW) to investigate its emergence in polymer chains. Using exact enumeration, we show that both the DJ model and ISAW exhibit negative energetic elasticity, which is caused by effective soft-repulsive interactions between polymer segments. Moreover, we find that a universal scaling law for the internal energy of both models, with a common exponent of $7/4$, holds consistently across both random-walk–self-avoiding-walk and self-avoiding-walk–neighbor-avoiding-walk crossovers. These findings suggest that negative energetic elasticity is a fundamental and universal property of polymer networks and chains.

Gels are soft solids containing large amounts of solvent. They are used in the production of everyday items such as jellies and soft contact lenses; for many applications, a particular elastic modulus is required. Conventionally, the shear modulus G of a gel is predicted using a classical rubber elasticity theory, such as the affine network [1], phantom network [2], or modified phantom network [3] model. These models assume that G is predominantly determined by entropic elasticity and therefore that G is approximately proportional to the absolute temperature (T) as $G \approx aT$. However, recent studies [4, 5] have discovered cases of negative energetic elasticity, in which $G = aT - b$ with a significantly large negative constant term $-b$ in some narrow range of temperature. Initially observed in hydrogels [4, 6, 7], negative energetic elasticity was subsequently confirmed in silicone gels [8] and calcium carbonate-based gels [9]. These findings have revealed a fundamental distinction between gels and rubbers: gels possess an intrinsic solvent-induced negative energetic contribution to the elasticity, whereas rubbers, lacking sufficient solvent content, do not. Thus, novel elastic theories beyond conventional paradigms aligning gel and rubber elasticity are needed.

Various theoretical approaches have been employed to understand the origin of negative energetic elasticity in gels, including lattice models [10–12] and all-atom molecular dynamics simulation [13]. Nevertheless, a concise and universally accepted explanation at the microscopic level remains elusive.

In this Letter, we investigate the microscopic origin of negative energetic elasticity by analyzing the Domb–Joyce (DJ) model [14–16], i.e., a simple extension of the random walk (RW) [Fig. 1(a)] with short-range repulsions introduced at the intersections along the polymer

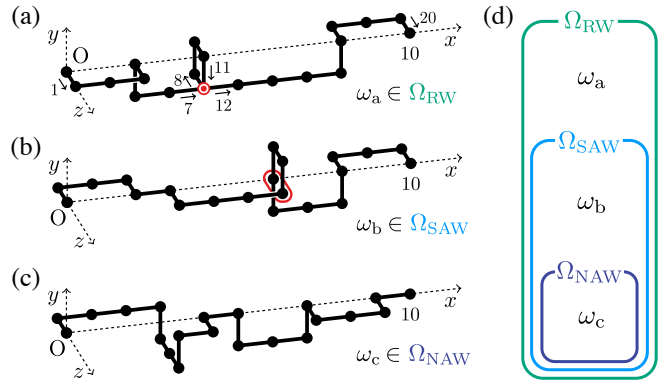


FIG. 1. Configurations of 20-step (a) random walk (RW) ω_a , (b) self-avoiding walk (SAW) ω_b , and (c) neighbor-avoiding walk (NAW) ω_c on cubic lattices with endpoints anchored at the origin and $(10, 0, 0)$. The red concentric circles in ω_a indicate a site occupied by two segments, and the red oval in ω_b highlights a pair of nearest-neighbor segments. (d) Inclusion relations $\Omega_{RW} \supset \Omega_{SAW} \supset \Omega_{NAW}$, where Ω_{RW} , Ω_{SAW} , and Ω_{NAW} are the configuration spaces of RWs, SAWs, and NAWs, respectively.

chain. As de Gennes has noted [17], the RW is “one of the simplest idealizations of a flexible polymer chain” and serves as a starting point for understanding polymer behavior. The DJ model reduces to the self-avoiding walk (SAW) [18, 19] [Fig. 1(b)] in the zero-temperature limit; therefore, it can be viewed as a bridge between the RW and SAW, and it has been used to explore the differences in their critical exponents. Recent studies have employed variations of the DJ model (extending from a self-interacting chain to a time series of a non-Markovian walker) to describe agents such as cells, animals, and active matter [20–24].

Through exact enumeration, we demonstrate that the DJ model exhibits negative energetic elasticity and provides a concise and intuitive interpretation of its origin in terms of the competition between the energetic and

* These authors contributed equally; Corresponding author. shirai@cc.mie-u.ac.jp

† These authors contributed equally; Corresponding author. sakumichi@gel.t.u-tokyo.ac.jp

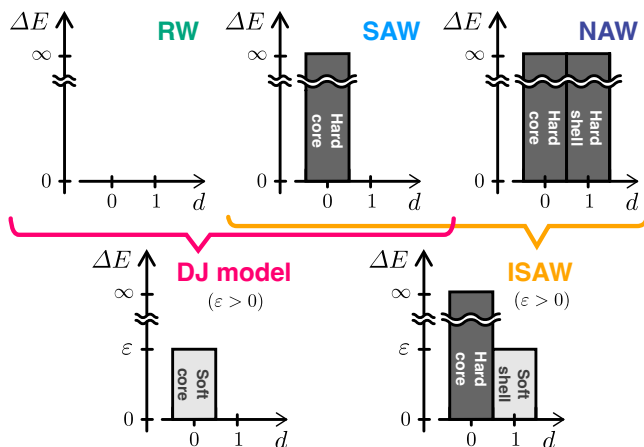


FIG. 2. Interaction energy (ΔE) in five lattice polymer models. The range of interactions is denoted by d ; when $d = 0$ or 1 , the interaction is between two segments occupying the same site or nearest-neighbor sites, respectively. The RW has no interactions between segments. The SAW introduces a hard-core repulsion ($d = 0$) that prohibits segment overlap. The NAW introduces an additional hard-shell repulsion ($d = 1$) between nearest-neighbor segments. The DJ model and the ISAW incorporate soft-core ($d = 0$) and soft-shell ($d = 1$) repulsions, respectively, with interaction strength $\varepsilon (> 0)$. Varying ε in these models allows continuous crossovers between the RW, SAW, and NAW.

entropic contributions to the elastic response. We compare the DJ model with the interacting self-avoiding walk (ISAW) [18, 25] used in Ref. [10] and suggest that any polymer chain possessing effective self-repulsive interactions between its segments exhibits negative energetic elasticity. Furthermore, we find a universal scaling law for the internal energy of both the DJ model and ISAW, with a common exponent of $7/4$. These findings suggest that negative energetic elasticity is a universal property of polymeric chains and networks, arising from the interplay between the chain's conformational entropy and the effective soft-repulsive interactions between its segments.

Models: RW–SAW and SAW–NAW crossovers.—We consider an n -step random walk (RW) on a simple cubic lattice with fixed endpoints $\omega(0) = (0, 0, 0)$ and $\omega(n) = (r, 0, 0)$, where r is the end-to-end distance ($r \geq 0$) and the lattice spacing is set to 1. The RW is defined by a sequence of sites $\omega = (\omega(0), \omega(1), \dots, \omega(n))$ satisfying $\omega(i) \in \mathbb{Z}^3$ and $|\omega(i+1) - \omega(i)| = 1$ for $i = 0, 1, \dots, n-1$. A self-avoiding walk (SAW) is defined as an RW that satisfies $\omega(i) \neq \omega(j)$ for all $i \neq j$ [19]. Figures 1(a) and 1(b) show configurations of a 20-step RW (ω_a) and SAW (ω_b), respectively.

To investigate the effects of short-range repulsive interactions on the elasticity of the polymer chains, we introduce the DJ model and ISAW [25] as extensions of the RW and SAW, respectively. Both models use a unified energy function for the repulsive interaction:

$$E(\omega) = \varepsilon m(\omega), \quad (1)$$

where $\varepsilon (> 0)$ is the repulsive interaction energy (bottom panels of Fig. 2), $m = m(\omega)$ is the number of interacting segment pairs, and ω is the configuration of the RW (SAW) for the DJ model (ISAW). In the DJ model, m increases whenever multiple segments occupy the same site. When $v (\geq 2)$ segments overlap at one site, m increases by the binomial coefficient $\binom{v}{2} \equiv v(v-1)/2$. In the ISAW, an interacting segment pair is defined as two sequentially nonadjacent segments occupying nearest-neighbor sites.

Figure 2 illustrates the interactions in five lattice polymer models, revealing the RW–SAW and SAW–NAW crossovers. The RW [Fig. 1(a)] has no interaction between its segments (top left of Fig. 2). The SAW [Fig. 1(b)] emerges from the RW when a hard-core repulsion is introduced (top center of Fig. 2) that prohibits segment overlap. The neighbor-avoiding walk (NAW) [Fig. 1(c)] emerges from the SAW when an additional hard-shell repulsion is introduced (top right of Fig. 2) [26]. The RW, SAW, and NAW all exhibit purely entropic elasticity; energetic elasticity is excluded because all configurations have identical energies. By contrast, the DJ model and ISAW introduce energy gradients via soft-core and soft-shell repulsions, respectively, with interaction energies $\varepsilon (> 0)$ (bottom panels of Fig. 2). By varying ε , the DJ model (ISAW) connects the RW (SAW) at $\varepsilon = 0$ to the SAW (NAW) at $\varepsilon = \infty$. These energy gradients enable the DJ model and ISAW to exhibit both energetic and entropic elasticities.

The energy function in Eq. (1) enables the DJ model and ISAW to be treated simultaneously as follows: The partition function under the on-axis constraint is given by

$$Z(r, \beta\varepsilon) = \sum_{m=0}^{m_{\text{ub}}} W_{n,m}(r) e^{-\beta\varepsilon m}, \quad (2)$$

where $\beta [\equiv 1/(k_B T)]$ is the inverse temperature, k_B is the Boltzmann constant, $W_{n,m}(r)$ is the number of possible configurations ω for given (n, r, m) , and m_{ub} is an upper bound on m . The free energy, internal energy, and entropy are given by $A(r, \beta\varepsilon) = -(1/\beta) \ln Z(r, \beta\varepsilon)$, $U(r, \beta\varepsilon) = \varepsilon \sum_{m=0}^{m_{\text{ub}}} m W_{n,m}(r) e^{-\beta\varepsilon m}$, and $S(r, \beta\varepsilon) = [A(r, \beta\varepsilon) - U(r, \beta\varepsilon)]/T$, respectively.

The finite-difference form of the stiffness for both models is given by

$$k(r, \beta\varepsilon) \equiv \frac{1}{\beta} \left[\left(\frac{1}{Z(r, \beta\varepsilon)} \sum_{m=0}^{m_{\text{ub}}} \frac{\Delta W_{n,m}(r)}{\Delta r} e^{-\beta\varepsilon m} \right)^2 - \frac{1}{Z(r, \beta\varepsilon)} \sum_{m=0}^{m_{\text{ub}}} \frac{\Delta^2 W_{n,m}(r)}{\Delta r^2} e^{-\beta\varepsilon m} \right], \quad (3)$$

where $\Delta W_{n,m}(r) \equiv [W_{n,m}(r + \Delta r) - W_{n,m}(r - \Delta r)]/2$ and $\Delta^2 W_{n,m}(r) \equiv W_{n,m}(r + \Delta r) - 2W_{n,m}(r) + W_{n,m}(r - \Delta r)$. Here, $\Delta r \equiv 2$ because ω exists only when r and n are both even or both odd. The stiffness k is the sum of energetic (k_U) and entropic (k_S) contributions, where $k_U(r, \beta\varepsilon) \equiv \partial^2 U(r, \beta\varepsilon)/\partial r^2$ and

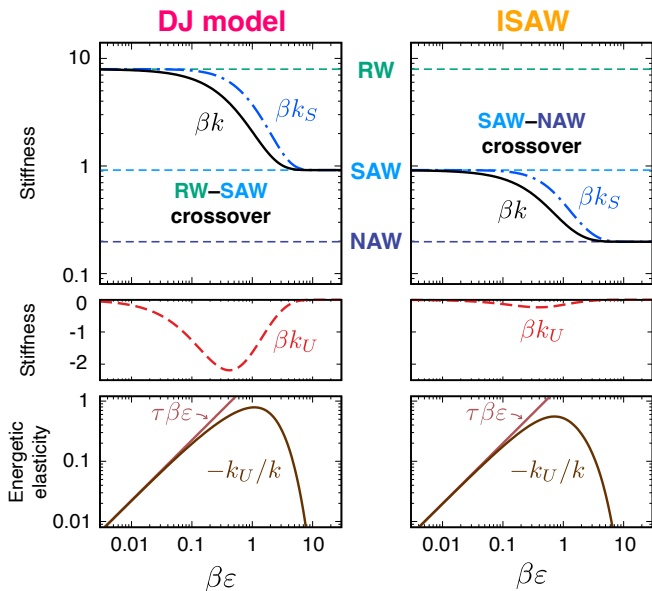


FIG. 3. Emergence of negative energetic elasticity in RW-SAW and SAW-NAW crossovers with $(n, r) = (20, 10)$. The DJ model bridges the RW and SAW (left column), and the ISAW bridges the SAW and NAW (right column). The data for the ISAW are obtained from Ref. [10]. The top panels show the dependence of total stiffness βk and the entropic contribution to stiffness βk_S on interaction strength $\beta\epsilon$. The middle panels show the energetic contribution to stiffness βk_U . The bottom panels show the ratio $-k_U/k$ and its first-order approximation $\tau\beta\epsilon$ around $\beta\epsilon = 0$. The maximum of $-k_U/k$ occurs around $\beta\epsilon \simeq 1$ for both models.

$k_S(r, \beta\epsilon) \equiv -T\partial^2 S(r, \beta\epsilon)/\partial r^2$. We use $k_S(r, \beta\epsilon) = -\beta\epsilon \partial k(r, \beta\epsilon)/\partial(\beta\epsilon)$, which is derived from Maxwell’s relations [1, 4, 5, 10], and $k_U = k - k_S$. When it is necessary to distinguish the models, we employ “RW” or “SAW” as superscripts on $W_{n,m}(r)$, and “DJ” and “ISAW” on other physical quantities.

Exact enumeration for the DJ model and ISAW.—We exactly enumerated $W_{n,m}^{\text{RW}}(r)$ for $n = 1, \dots, 20$, $W_{n,m}^{\text{RW}}(n-8)$ for $n = 21, 22, 23$, $W_{n,m}^{\text{RW}}(n-10)$ for $n = 21, \dots, 26$, and $W_{n,m}^{\text{SAW}}(n-10)$ for $n = 21, \dots, 29$, using the simplest recursive algorithm [27] with two pruning algorithms. Here, we considered the octahedral symmetry of the simple cubic lattice and the reachability of ω to an endpoint on the x -axis (the method is explained in Sec. S2 of Ref. [10]). These results are consistent with those reported in Refs. [10, 28–34].

Polynomials in arbitrary n of $W_{n,m}^{\text{RW}}(r)$ and $W_{n,m}^{\text{SAW}}(r)$.—Using the enumerated $W_{n,m}^{\text{RW}}(r)$ and $W_{n,m}^{\text{SAW}}(r)$, we derived the polynomials in positive integer n that exactly reproduced the numbers $W_{n,m}^{\text{RW}}(r)$ and $W_{n,m}^{\text{SAW}}(r)$ for $r = n, n-2, n-4, n-6, n-8$, and $n-10$. These polynomials enable the calculation of any physical quantity derived from Eq. (2) for $0 \leq n-r \leq 10$.

Emergence of negative energetic elasticities in lattice polymer chains.—As shown in Fig. 3, the two crossovers

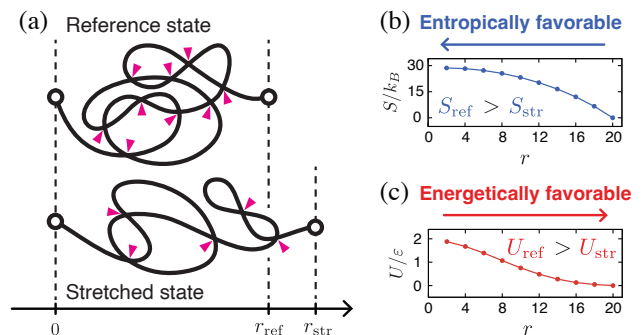


FIG. 4. Intuitive interpretation of the emergence of negative energetic elasticity originating from the entropy–energy interplay. (a) The reference state with end-to-end distance $r = r_{\text{ref}} (> 0)$ is entropically favorable (top), whereas the stretched state with $r = r_{\text{str}} (> r_{\text{ref}})$ is energetically favorable (bottom) because it has fewer intersections. This interpretation is consistent with the behavior of (b) the entropy $S_n^{\text{DJ}}(r, \beta\epsilon)$ and (c) the internal energy $U_n^{\text{DJ}}(r, \beta\epsilon)$, which are monotonically decreasing functions of r for $1 \leq r \leq 20$. Here, we set $\beta\epsilon = 1$ and $n = 20$.

interconnecting the RW, SAW, and NAW ($\beta k_U = 0$) reveal that both the DJ model and ISAW exhibit negative energetic elasticity ($\beta k_U < 0$) with $|k_U/k|$ maximized around $\beta\epsilon \sim 1$. For $(n, r) = (20, 10)$ and the same $\beta\epsilon$, k^{DJ} is 4.6 to 8.7 times larger than k^{ISAW} because the configuration space of the RW is larger than that of the SAW. The ratio of $|(k_U/k)^{\text{DJ}}|$ to $|(k_U/k)^{\text{ISAW}}|$ ranges from 1.1 to 2.7, demonstrating the enhanced negative energetic elasticity in the DJ model compared to that in the ISAW.

The soft repulsions between polymer segments in the DJ model and ISAW (Fig. 2) are the microscopic origin of the negative energetic elasticity observed in Fig. 3. Our results suggest that any polymer chain, whether alone [35–37] or in a network [38, 39], can exhibit negative energetic elasticity if it possesses effective self-repulsion between polymer segments.

The DJ model provides an intuitive interpretation of the emergence of negative energetic elasticity. The stiffness at $r = 10$ shown in Fig. 3 is calculated from the differences in the free energy at $r = 8, 10$, and 12. Therefore, to elucidate the underlying mechanism, we consider the r -dependence of both entropy and internal energy. Figure 4(a) illustrates two configurations of a coarse-grained polymer chain with soft-core repulsion: a reference state and a stretched state. The energy increases at intersections within the chains [pink triangles in Fig. 4(a)]. The stretched state, which possesses fewer intersections, is thus energetically favorable compared to the reference state. This property holds for the ensemble of chain configurations: states with longer end-to-end distances are energetically favorable; those with shorter end-to-end distances are entropically favorable. This behavior is demonstrated by the monotonic decrease of both the entropy $S_n^{\text{DJ}}(r, \beta\epsilon)$ [Fig.4(b)] and the internal energy

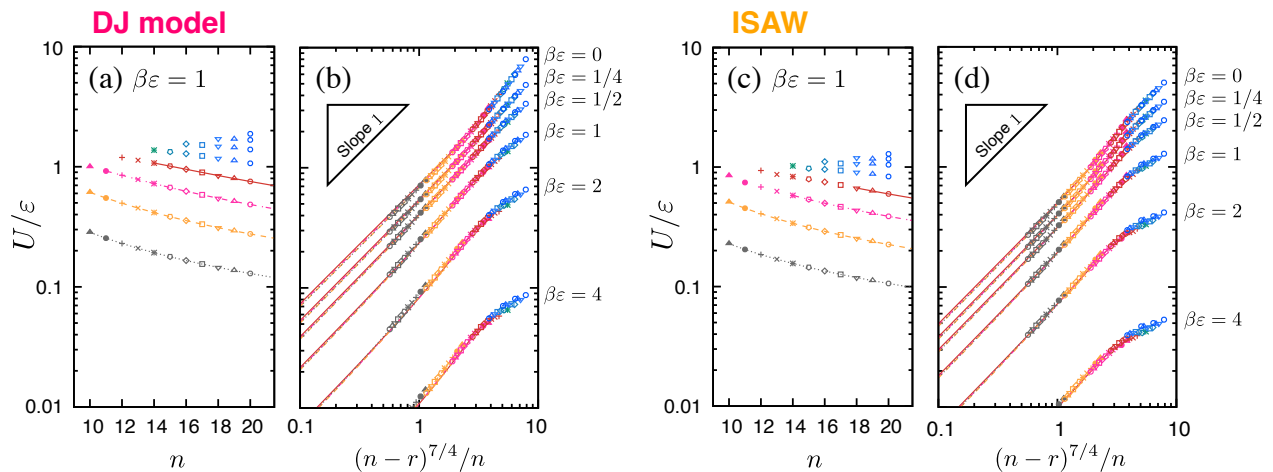


FIG. 5. Universal scaling of the internal energy $U_n(r, \beta\epsilon)/\epsilon$ for (a,b) the DJ model across RW–SAW crossover and (c,d) the ISAW across SAW–NAW crossover. In each panel, points correspond to $n = 10, 11, \dots, 20$ and $2 \leq r \leq n - 4$; curves represent the four analytic expressions for $U_n(r, \beta\epsilon)/\epsilon$ obtained from the polynomials of $W_{n,m}^{\text{RW}}(r)$ and $W_{n,m}^{\text{SAW}}(r)$ for $r = n - 4$ (gray), $n - 6$ (orange), $n - 8$ (pink), and $n - 10$ (red). In (a,c), $\beta\epsilon = 1$; for a fixed n , $U_n(r, \beta\epsilon)/\epsilon$ monotonically decreases with increasing r . In (b,d), $U_n(r, \beta\epsilon)/\epsilon$, plotted against the scaled variable $(n - r)^{7/4}/n$, collapses onto master curves with a common scaling exponent $7/4$ for a wide range of interaction strengths ($\beta\epsilon = 0, 1/4, 1/2, 1, 2, \text{ and } 4$). The master curves in the log–log plots exhibit slopes close to 1, indicating an almost linear relation between $U_n(r, \beta\epsilon)/\epsilon$ and $(n - r)^{7/4}/n$.

$U_n^{\text{DJ}}(r, \beta\epsilon)$ [Fig. 4(c)] with increasing r . This interplay between energetic and entropic factors gives rise to negative energetic elasticity.

Scaling in internal energy.—Figures 5(a) (DJ model) and 5(c) (ISAW) show the exact values of $U_n(r, \beta\epsilon)/\epsilon$ as a function of the chain length n for $n = 10, 11, \dots, 20$ and $\beta\epsilon = 1$. Here, the end-to-end distance range is $2 \leq r \leq n - 4$. Also shown are four analytic expressions for $U_n(r, \beta\epsilon)/\epsilon$ corresponding to $r = n - 4, n - 6, n - 8$, and $n - 10$. Remarkably, when plotted against the scaled variable $(n - r)^{7/4}/n$, the data points and analytic expressions for $U_n(r, \beta\epsilon)/\epsilon$ collapse onto a single master curve for both the DJ model [Fig. 5(b)] and ISAW [Fig. 5(d)] across the entire range of the two crossovers ($\beta\epsilon = 0, 1/4, 1/2, 1, 2, \text{ and } 4$). The master curves exhibit almost linear behavior, suggesting that $U_n(r, \beta\epsilon)/\epsilon \propto (n - r)^{7/4}/n$ can be used as a practical approximation.

The component $n - r$ appearing in the scaling variable $(n - r)^{7/4}/n$ is the “slack” of the chain, i.e., the number of segments remaining after assigning r segments in the $+x$ -direction to reach the endpoint $(r, 0, 0)$. That a common exponent $7/4$ emerges from the DJ model and the ISAW suggests that this exponent is universal and depends only on the spatial dimensions of the system. Remarkably, the scaling of the internal energy based on the slack $n - r$ is consistent with the scaling of τ^{ISAW} found in Ref. [10], which exhibits an exponent of $3/4$. Here, $\tau \equiv [\partial/\partial(\beta\epsilon)](-k_U/k)|_{\beta\epsilon=0}$ is the first-order coefficient in the Taylor expansion of $-k_U/k$ with respect to $\beta\epsilon$ (see bottom panels of Fig. 3); Ref. [10] uses the notation T_U^∞ instead of τ . The exponent $3/4$ coincides with the well-established universal critical exponent $\nu = 3/4$ of the two-dimensional SAW [40, 41]. This coincidence sug-

gests a possible reduction from three to two dimensions induced by the on-axis constraint on the end-to-end vector (see Sec. S8 in Supplemental Materials of Ref. [10]). Furthermore, the simple relationship between the exponents (i.e., $7/4 = 3/4 + 1$) can potentially be explained by introducing a scaling function similar to that of the Widom scaling hypothesis [42, 43]. The analysis of the DJ model under the on-axis constraint presented here is expected to advance the long-standing effort, dating back to the 1970s [14], to connect the critical exponents of the three-dimensional RW and SAW [44].

Conclusion—We elucidated the microscopic origin of negative energetic elasticity in polymer chains using the DJ model and ISAW. Our investigation of the two crossovers among the RW, SAW, and NAW (Fig. 3) revealed that effective soft-repulsive interactions between polymer segments are the origin of the negative energetic elasticity of flexible polymers. The DJ model provides an intuitive interpretation (Fig. 4): longer end-to-end distances are energetically favorable, whereas shorter distances are entropically favorable. We also discovered a universal scaling with an exponent of $7/4$ for the internal energy of both models throughout the crossovers (Fig. 5). This intuitive interpretation of the negative energetic elasticity is expected to serve as a guideline for further theoretical development and material design.

ACKNOWLEDGMENTS

We thank Kazutaka Takahashi for his insightful comments on the critical exponents. This study was supported by JSPS KAKENHI Grant No. JP22K13973 to

-
- [1] P. J. Flory, *Principles of Polymer Chemistry* (Cornell University Press, Ithaca, 1953).
- [2] H. M. James and E. Guth, Theory of the elastic properties of rubber, *J. Chem. Phys.* **11**, 455 (1943).
- [3] M. Zhong, R. Wang, K. Kawamoto, B. D. Olsen, and J. A. Johnson, Quantifying the impact of molecular defects on polymer network elasticity, *Science* **353**, 1264 (2016).
- [4] Y. Yoshikawa, N. Sakumichi, U. Chung, and T. Sakai, Negative energy elasticity in a rubberlike gel, *Phys. Rev. X* **11**, 011045 (2021).
- [5] N. Sakumichi, Y. Yoshikawa, and T. Sakai, Linear elasticity of polymer gels in terms of negative energy elasticity, *Polym. J.* **53**, 1293 (2021).
- [6] T. Fujiyabu, T. Sakai, R. Kudo, Y. Yoshikawa, T. Katashima, U. Chung, and N. Sakumichi, Temperature dependence of polymer network diffusion, *Phys. Rev. Lett.* **127**, 237801 (2021).
- [7] J. Tang, R. H. Colby, and Q. Chen, Revisiting the elasticity of tetra-poly(ethylene glycol) hydrogels, *Macromolecules* **56**, 2939 (2023).
- [8] T. Aoyama and K. Urayama, Negative and positive energetic elasticity of polydimethylsiloxane gels, *ACS Macro Lett.* **12**, 356 (2023).
- [9] X. Liu, K. Kong, J. Wang, Z. Liu, and R. Tang, Molecular weight-dependent physicochemical behaviors of calcium carbonate chains, *J. Phys. Chem. Lett.* **15**, 5905 (2024).
- [10] N. C. Shirai and N. Sakumichi, Solvent-induced negative energetic elasticity in a lattice polymer chain, *Phys. Rev. Lett.* **130**, 148101 (2023).
- [11] L. K. Duarte and L. G. Rizzi, On the origin of the negative energy-related contribution to the elastic modulus of rubber-like gels, *Eur. Phys. J. E* **46**, 52 (2023).
- [12] A. Iwaki and S. Ozaki, Solvable toy model of negative energetic elasticity, arXiv:2404.06885.
- [13] K. Hagita, S. Nagahara, T. Murashima, T. Sakai, and N. Sakumichi, All-atom molecular dynamics simulations of poly(ethylene glycol) networks in water for evaluating negative energetic elasticity, *Macromolecules* **56**, 8095 (2023).
- [14] C. Domb and G. S. Joyce, Cluster expansion for a polymer chain, *J. Phys. C* **5**, 956 (1972).
- [15] C. Domb, From random to self-avoiding walks, *J. Stat. Phys.* **30**, 425 (1983).
- [16] G. Slade, Self-avoiding walk, spin systems and renormalization, *Proc. R. Soc. A* **475**, 20180549 (2019).
- [17] P. G. de Gennes, *Scaling Concepts in Polymer Physics* (Cornell University Press, Ithaca, 1979), Sec. I.1.1 Simple random walks, p. 29.
- [18] W. J. Orr, Statistical treatment of polymer solutions at infinite dilution, *Trans. Faraday Soc.* **43**, 12 (1947).
- [19] N. Madras and G. Slade, *The Self-Avoiding Walk* (Birkhäuser, Boston, 1996), 10.1007/978-1-4612-4132-4.
- [20] T. Guérin, N. Levernier, O. Bénichou, and R. Voituriez, Mean first-passage times of non-markovian random walkers in confinement, *Nature* **534**, 356 (2016).
- [21] P. Grassberger, Self-trapping self-repelling random walks, *Phys. Rev. Lett.* **119**, 140601 (2017).
- [22] J. d'Alessandro, A. Barbier-Chebbah, V. Cellerin, O. Bénichou, R. M. Mège, R. Voituriez, and B. Ladoux, Cell migration guided by long-lived spatial memory, *Nat. Commun.* **12**, 1 (2021).
- [23] A. Barbier-Chebbah, O. Bénichou, and R. Voituriez, Self-interacting random walks: Aging, exploration, and first-passage times, *Phys. Rev. X* **12**, 011052 (2022).
- [24] L. Régnier, M. Dolgushev, and O. Bénichou, From maximum of inter-visit times to starving random walks, *Phys. Rev. Lett.* **132**, 127101 (2024).
- [25] C. Vanderzande, *Lattice Models of Polymers* (Cambridge University Press, Cambridge, England, 1998), 10.1017/CBO9780511563935.
- [26] T. Ishinabe and Y. Chikahisa, Exact enumerations of self-avoiding lattice walks with different nearest-neighbor contacts, *J. Chem. Phys.* **85**, 1009 (1986).
- [27] J. L. Martin, The exact enumeration of self-avoiding walks on a lattice, *Math. Proc. Cambridge Philos. Soc.* **58**, 92 (1962).
- [28] C. Domb, On the theory of cooperative phenomena in crystals, *Adv. Phys.* **9**, 245 (1960).
- [29] C. Domb, J. Gillis, and G. Wilmers, On the shape and configuration of polymer molecules, *Proc. Phys. Soc. London* **85**, 625 (1965).
- [30] G. S. Joyce, On the simple cubic lattice green function, *Philos. Trans. R. Soc. London* **273**, 583 (1973).
- [31] P. Butera and M. Comi, Critical specific heats of the n-vector spin models on the simple cubic and bcc lattices, *Phys. Rev. B* **60**, 6749 (1999).
- [32] S. Hollos, Lattice Paths and Walks, <https://www.exstrom.com/math/lattice/latpath.html> (2007).
- [33] N. J. A. Sloane, Entry A002896 in The On-Line Encyclopedia of Integer Sequences, <https://oeis.org/A002896> (2023).
- [34] S. Hollos, Entry A135390 in The On-Line Encyclopedia of Integer Sequences, <https://oeis.org/A135390> (2023).
- [35] A. Janshoff, M. Neitzert, Y. Oberdörfer, and H. Fuchs, Force spectroscopy of molecular systems—single molecule spectroscopy of polymers and biomolecules, *Angew. Chem. Int. Ed.* **39**, 3212 (2000).
- [36] W. Zhang and X. Zhang, Single molecule mechanochemistry of macromolecules, *Prog. Polym. Sci.* **28**, 1271 (2003).
- [37] Y. Bao, Z. Luo, and S. Cui, Environment-dependent single-chain mechanics of synthetic polymers and biomacromolecules by atomic force microscopy-based single-molecule force spectroscopy and the implications for advanced polymer materials, *Chem. Soc. Rev.* **49**, 2799 (2020).
- [38] Y. Gu, J. Zhao, and J. A. Johnson, Polymer networks: From plastics and gels to porous frameworks, *Angew. Chem. Int. Ed.* **59**, 5022 (2020).
- [39] S. Nakagawa and N. Yoshie, Star polymer networks: a toolbox for cross-linked polymers with controlled structure, *Polym. Chem.* **13**, 2074 (2022).
- [40] B. Nienhuis, Exact critical point and critical exponents

- of $O(n)$ models in two dimensions, *Phys. Rev. Lett.* **49**, 1062 (1982).
- [41] B. Nienhuis, Critical behavior of two-dimensional spin models and charge asymmetry in the coulomb gas, *J. Stat. Phys.* **34**, 731 (1984).
- [42] B. Widom, Equation of state in the neighborhood of the critical point, *J. Chem. Phys.* **43**, 3898 (1965).
- [43] J. Cardy, *Scaling and Renormalization in Statistical Physics* (Cambridge University Press, Cambridge, England, 1996), Sec. 3.4 Scaling behaviour of the free energy, p. 43, 10.1017/CBO9781316036440.
- [44] P. Grassberger, P. Sutter, and L. Schäfer, Field theoretic and Monte Carlo analysis of the Domb–Joyce model, *J. Phys. A* **30**, 7039 (1997).